Volume 3, Issue 5, May 2013 ISSN: 2277 128X
International Journal of Advanced Research in Computer Science and Software Engineering
Research Paper
Available online at: www.ijarcsse.com

The Analytical Investigation of the effect of wind farm equipped with SCIG on static voltage stability by a new index

Hamid Reza Najafi Mahmoud Ebadian Mostafa Vahedipour Dahraie*
Department of Electrical Engineering, University of Birjand, Birjand, Iran.

Abstract— In this paper, the effect of wind farm equipped with SCIG on the static voltage stability of the power system is investigated analytically. To achieve this objective, the active and reactive output power of wind farm have been obtained at wind speed and generator terminal voltage. By using an appropriate model for SCIG and by linking the wind farm to a simple two-bus power system, the bus load voltage has been calculated. By calculating deflection point at different wind speeds, the maximum loading curve of the system at wind speed is obtained. This curve shows the stable and unstable regions of the system at different wind speeds. In order to obtain an appropriate criterion for the effect of wind farm on the static voltage stability, a new index has been introduced and by using it the effect of wind farm on static voltage stability is investigated.

Keywords— wind farm, squirrel cage induction generator (SCIG), voltage stability, static voltage stability

I. INTRODUCTION

Nowadays, using wind power generating systems in electricity networks of the world is increasing rapidly [1]. The increase of the penetration of wind power in network has a considerable impact on stability of power systems [2,3]. Since the squirrel cage induction generators are used in many of the wind turbines [4], and since these units are incapable of generating reactive power, therefore, they cause serious problems in voltage stability of the network [5]. The effect of wind farm on long-term and short-term voltage stability has been intensively investigated in several papers [2,3], [6]-[9]. In this paper, static voltage stability of the network in presence of wind farm is analyzed by introducing a new index. At first, in section 2 the study system is introduced, and an appropriate model for induction generator is presented, through which the wind farm is modeled as a PQ Bus in order to be used in load flow analysis. In section 3, the system's voltage stability conditions in presence of wind farm is investigated. In this regards, a suitable novel index is defined to calculate the effect of wind farm on voltage stability of the. The effect of various factors on static voltage stability can be investigated by proposed. In section 4, the conclusion of the paper is given.

II. THE STUDY SYSTEM MODELING

The general system configuration is shown in Fig.1. The under-study wind farm includes 30 wind turbine units equipped with SCIG which has been modeled by an equivalent wind turbine, and has been connected to a transmission network through two transformers. Parameters of induction generator and equivalent wind turbine are given in appendix.

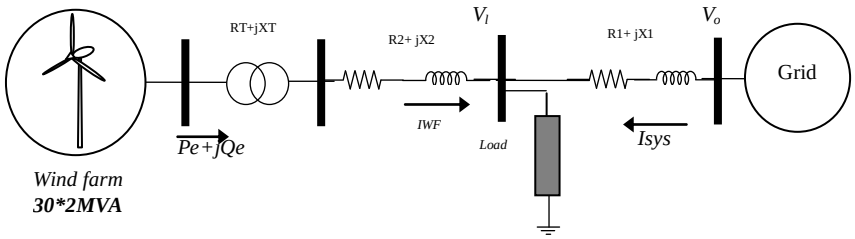

Fig. 1. Single line diagram of the study system

A. Model of Wind Power Generation System

Fig.2 shows the wind power generation system which includes turbine, blades, SCIG, gearbox, etc.

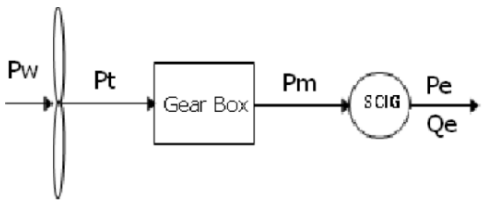

Fig. 2. Wind power generation system

Regarding Fig. 2, P_W is wind power, and P_t is converted turbine power which is obtained from equations (1) and (2) respectively.

$$P_W = 0.5\rho AV^3 \quad (1)$$

$$P_t = 0.5C_P(\lambda,\beta)\rho AV^3 \quad (2)$$

Where ρ is air density, A is swept surface by the blades, V is wind speed, and $C_P(\lambda,\beta)$ is turbine function coefficient which are obtained from following equations:

$$C_P(\lambda,\beta) = c_1\left(\frac{c_2}{\lambda_1} - c_3\beta - c_4\right)e^{\frac{-c_5}{\lambda_i}} + c_6\lambda \quad (3)$$

$$\frac{1}{\lambda_i} = \frac{1}{\lambda + 0.008} - \frac{0.035}{\beta^3 + 1} \quad (4)$$

$$\lambda = \frac{R\omega}{V} \quad (5)$$

In above equations, λ is speed ratio of tip of blade, ω is the angular speed of rotor, and β is the blade angle. c_i s ($i = 1,2,...,6$) are turbine constants.

The converted power of turbine which is decreased partly in mechanical part is applied to rotor generator as mechanical power.

$$P_m = \eta_m P_t \quad (6)$$

Where η_m is mechanical part efficiency.

B. Induction Generator Model

No Different model for studying steady-state conditions of induction generator are presented in different papers [10]-[13]. In this section induction generator is modeled as shown in Fig. 3.

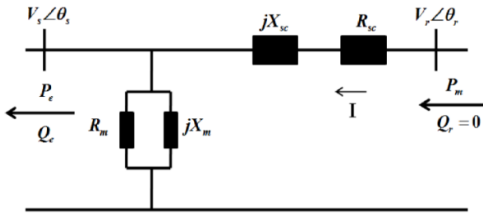

Fig. 3 The steady state model of squirrel cage induction generator

In this model, rotor parameters are referred to stator side. Here, $V_s\angle\theta_s$ and $V_r\angle\theta_r$ are the referred stator and rotor voltages respectively. R_{sc} is the referred stator and rotor equivalent resistance. X_{sc} is the referred stator and equivalent reactance. R_m and X_m are the core loss and magnetizing reactance of generator respectively.

Using this model we have:

$$I = \frac{P_m}{V_r\angle -\theta_r} \quad (7)$$

$$V_s\angle\theta_s = V_r\angle\theta_r - (R_{sc} + jX_{sc}).I \quad (8)$$

By substituting equation (7) into (8) and simplifying it a little, (9) is achieved.

$$V_r = \left[\frac{2R_{sc}P_m + V_s^2 + \sqrt{V_s^4 + 4P_m R_{sc}V_s^2 - 4P_m^2 X_{sc}^2}}{2}\right]^{0.5} \quad (9)$$

Active and reactive power of generator can be obtained from the following equations:

$$P_e = P_m - R_{sc}\frac{P_m^2}{V_R^2} - \frac{V_s^2}{R_m} \quad (10)$$

$$Q_e = -X_{sc}\frac{P_m^2}{V_r^2} - \frac{V_s^2}{X_m} \quad (11)$$

By placing (9) into (10) and (11), we have:

$$P_e = P_m - \frac{V_s^2}{R_m} - \frac{2R_{sc}P_m^2}{V_s^2 + 2R_{sc}P_m + \sqrt{V_s^4 + 4P_m R_{sc}V_s^2 - 4P_m^2 X_{sc}^2}} \quad (12)$$

$$Q_e = -\frac{V_s^2}{X_m} - \frac{2X_{sc}P_m^2}{V_s^2 + 2R_{sc}P_m + \sqrt{V_s^4 + 4P_m R_{sc}V_s^2 - 4P_m^2 X_{sc}^2}} \quad (13)$$

By substituting P_m from equation (6) into (12) and (13), active and reactive power of generator can be obtained as a function of wind speed and terminal voltage. Fig. 4 shows the active and reactive power curves of the wind farm with respect to wind speed. In this model, the injected reactive power to the network is negative. Here, the cut_{in}, nominal and cut_{out} wind speed are 4, 16, and 25 m/s respectively.

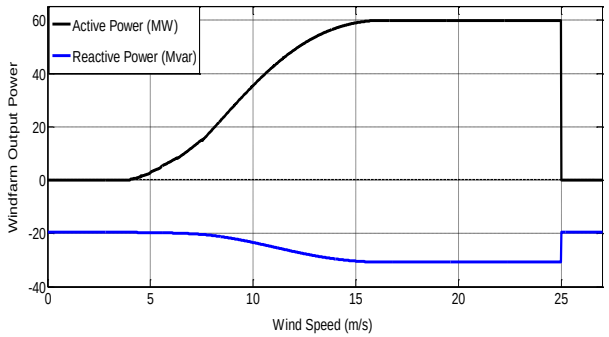

Fig.4. Output power of the wind farm

P_{WF} and Q_{WF} are the active and reactive power of the wind farm respectively which are injected to the load bus and can be obtained from (14) and (15).

$$P_{WF} = P_e - R_{WF}I_{WF}^2 \quad (14)$$

$$Q_{WF} = Q_e - X_{WF}I_{WF}^2 \quad (15)$$

In above equations we have:

$$I_{WF} = \frac{P_{WF} - jQ_{WF}}{V_l^*} \quad (16)$$

$$R_{WF} = R_T + R_2 \quad (17)$$

$$X_{WF} = X_T + X_2 \quad (18)$$

$$I_{sys} = I_l - I_{WF} \quad (19)$$

$$I_l = \frac{P_l - jQ_l}{V_l\angle -\theta_l} \quad (20)$$

By replacing I_{WF} and I_l from equations (16) and (20) into (19),

$$I_{sys} = \frac{(P_l - P_{WF}) - (jQ_l - Q_{WF})}{V_l\angle -\theta_l} \quad (21)$$

By writing KVL in Fig. 1 we have:

$$V_0\angle 0 = V_1\angle\theta_l + (R_1 + jX_1)I_{sys} \quad (22)$$

$$V_0\angle 0 = V_l\angle\theta_l + (R_1 + jX_1).\left(\frac{(P_l - P_{WF}) - j(Q_l - Q_{WF})}{V_l\angle -\theta_1}\right) \quad (23)$$

After simplifying (23), equation (24) is achieved for V_l:

$$V_l = \{V_0^2 - [(Q_l - Q_{WF}).X_l + (P_l - P_{WF}).R_1] \pm \sqrt{V_0^4 - [(Q_l - Q_{WF}).X_1 + (P_l - P_{WF}).R_1].V_0^2 - 4[(P_l - P_{WF}).X_1 - (Q_l - Q_{WF}).R_1]^2}\}^{0.5} \quad (24)$$

Where in above equation, P_{WF} and Q_{WF} can be achieved from equations (14) and (15). Therefore, load bus voltage is achieved as a function of wind speed, bus load, wind farm and power system parameters. To calculate the maximum active power of the system in presence of wind farm, $P_{\max WF}$, we differentiate equation (24) by assuming that the reactive load power and wind farm reactive power are constant.

$$P_{\max WF} = \frac{(Q_l - Q_{WF})R_1}{X_1} - \frac{V_0^2 R_1}{2X_1^2} + \frac{|Z_{L1}|V_0\sqrt{V_0^2 - 4(Q_l - Q_{WF})X_1}}{2X_1^2} \quad (25)$$

Similarly, to calculate the maximum reactive power of the system in presence of wind farm, $Q_{\max WF}$, we differentiate equation (24) for a constant reactive load power and specified wind farm power.

$$Q_{\max WF} = \frac{(P_l - P_{WF})X_1}{R_1} - \frac{V_0^2 X_1}{2R_1^2} + \frac{|Z_{L1}|V_0\sqrt{V_0^2 - 4(P_l - P_{WF})R_1}}{2R_1^2} \quad (26)$$

Above equation, $Z_{L1} = \sqrt{R_1^2 + X_1^2}$.

By placing Q_{WF} from equation (15) in equation (25), $P_{\max WF}$ is obtained at wind farm parameters. similarly by placing P_{WF} from equation (14) in equation (26), $Q_{\max WF}$ is obtained at wind farm parameters.

III. INVESTIGATING THE EFFECT OF WIND FARM ON STATIC VOLTAGE STABILITY

In this section, the effect of wind farm on static voltage stability is investigated. To achieve this objective, the maximum system loading before and after connecting wind farm at different wind speeds has been calculated. In this regard, the system load is increased according to equation (27) with an increasing coefficient named loading parameter, (λ), from the base load, (P_{l0}). The load power factor is assumed constant and considered 0.9 lag in this study.

$$P_l = P_{l0}(1 + \lambda) \quad (27)$$

The maximum λ where the system reaches its unstable region is shown as $\lambda_{\max}$ and is called system's maximum loading parameter.

Fig.5 shows the system's maximum loading parameter curve (MLPC) at different wind speeds. It can be observed that the maximum load that the system can provide before vanishing depend on wind speed. The area under MPLC shows the stable region. In fig. 6 The maximum loading of the system in presence of wind farm has been compared with the maximum loading of the system without wind farm, ($\lambda_{\max} = 2.277$). The presence of wind farm in these conditions causes the weakening of the system in terms of static voltage stability. The effect of wind farm on voltage stability depends on various parameters. For investigating the effect of such parameters it is necessary to first define an appropriate index which shows the effect of wind farm on static voltage stability.

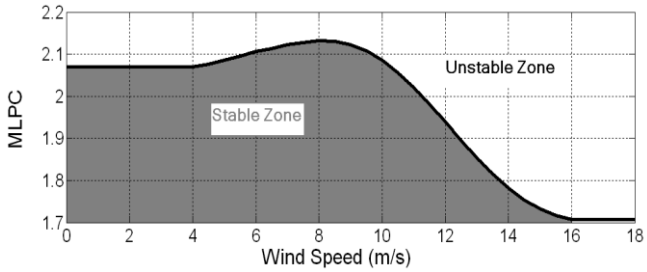

Fig.5. maximum loading curve of system at different wind speeds

A. *Definition of a New Index for Calculating the Effect of Wind Farm on Static Voltage Stability*

Fig. 6 shows that the presence of wind farm causes the maximum system loading to vary as a function of $\lambda_{\max WF} - \lambda_{\max}$, where $\lambda_{\max WF}$ is the maximum system loading in presence of wind farm.

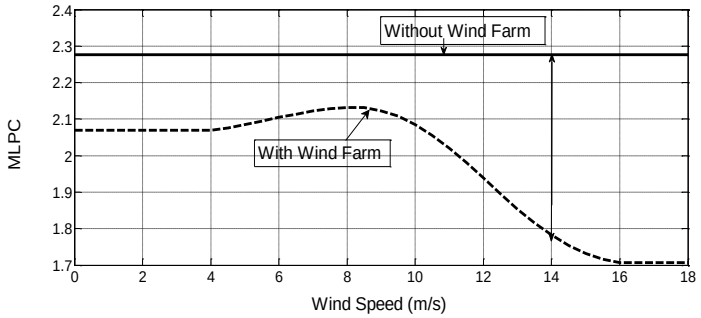

Fig.6. The difference of maximum system loading with and without wind farm

The normalized maximum system loading before and after connecting wind farm can be defined as a new index. The index of wind farm effect on voltage stability of the system is defined as:

$$WFVSI = \frac{\lambda_{\max WF} - \lambda_{\max}}{\lambda_{\max}} \tag{28}$$

Where $\lambda_{\max}$ and $\lambda_{\max WF}$ are achieved from equations (29) and (30), respectively

$$\lambda_{\max} = \min\{\frac{P_{\max} - P_0}{P_0}, \frac{Q_{\max} - Q_0}{Q_0}\} \tag{29}$$

$$\lambda_{\max WF} = \min\{\frac{P_{\max WF} - P_0}{P_0}, \frac{Q_{\max WF} - Q_0}{Q_0}\} \tag{30}$$

In a power system, static voltage stability occurs at first, unless the system has sufficient reactive power. Therefore, equations (31) and (32) can be considered for $\lambda_{\max}$ and $\lambda_{\max WF}$.

$$\lambda_{\max} = \frac{Q_{\max} - Q_0}{Q_0} \tag{31}$$

$$\lambda_{\max WF} = \frac{Q_{\max WF} - Q_0}{Q_0} \tag{32}$$

By replacing equations (31) and (32) in equation (28) we have:

$$WFVSI = \frac{Q_{\max WF} - Q_{\max}}{Q_{\max} - Q_0} \tag{33}$$

The critical reactive power of the system without wind farm, $Q_{\max}$, is:

$$Q_{\max} = \frac{P_1 X_1}{R_1} - \frac{V_s^2 X_1}{2R_1^2} + \frac{|Z_{L1}| V_s \sqrt{V_s - 4P_1 R_1}}{2R_1^2} \tag{34}$$

By substituting (26) and (34) in (33) and after simplifing, we have:

$$WFVSI = \frac{P_{WF} X_1 + |Z_{L1}| V_0 (\frac{\sqrt{V_0 - 4(P_1 - P_{WF})R_1}}{2R_1} - \frac{\sqrt{V_0 - 4P_1 R_1}}{2R_1}}{P_1 X_1 - \frac{V_0^2 X_1}{2R_1} + \frac{\sqrt{V_0 - 4P_1 R_1}}{2R_1} - R_1 Q_1} \tag{35}$$

Now, by substituting P_{WF} from (14) in (35), WFVSI is achieved versus wind farm parameters and system parameters. Therefore, by using (35), we can analyze the effect of different parameters on static voltage stability of the system.

WFVSI can be positive, negative, or zero. If WFVSI becomes positive; it means that the presence of wind farm has caused the system to become unstable at higher loading, in other words, the effect of wind farm on static voltage stability is positive. If WFVSI is negative; it means that the presence of wind farm has deteriorated the static voltage stability of the system, causing the system to become unstable at lower loading. If WFVSI approaches zero; it means that wind farm has no effect on static voltage stability of the system.

In this index, the larger positive number indicates more positive impact, and the larger negative number indicates more negative impact.

Fig. 7 shows WFVSI for the study system. In this condition, the index is negative for all the wind speeds. It means that wind farm in this condition has had negative impact on voltage stability, particularly, at speeds close to nominal wind speed it has caused even more instability in system voltage.

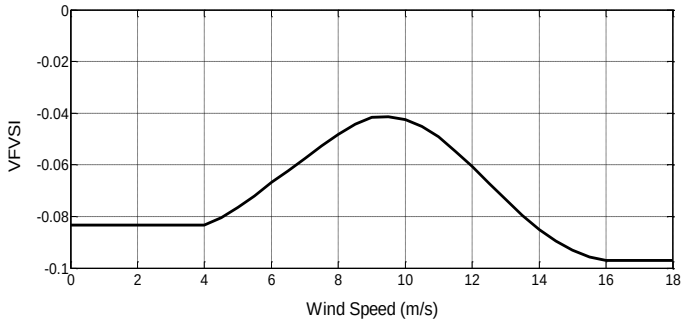

Fig. 7. WFVSI for the under-study system

Regarding equation (33) we can write:

$$WFVSI = \frac{\frac{Q_{\max WF} - Q_{\max}}{Q_0}}{\frac{Q_{\max} - Q_0}{Q_0}} = \frac{Q_{\max WF} - Q_{\max}}{Q_0 . \lambda_{\max}} \tag{36}$$

Therefore, we have:

$$Q_{\max WF} - Q_{\max} = WFVSI . Q_0 . \lambda_{\max} \tag{37}$$

The difference between critical reactive power with and without wind farm is shown with another index, named WFRPI index. Therefore, we have:

$$WFRPI = WFVSI . Q_0 . \lambda_{\max} \tag{38}$$

This index shows that by connecting wind farm to the network how much reactive power is necessary to neutralize the negative impact of connecting wind farm or how much reactive power must be added to reactive power of the network.

WFRPI is shown in fig.8 for the study system. This index provides the owners of wind farm and network operator with an appropriate sight for reactive power compensation.

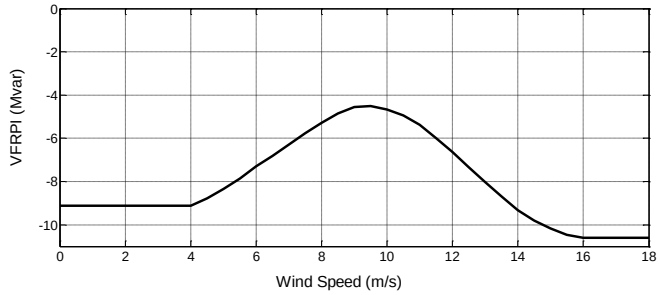

Fig. 8. WFRPI for the under-study system

B. *Induction Generat Investigating the effect of different wind farm parameters on static voltage stability*

Now that appropriate indexes were achieved for the assessment of static voltage stability of the system in presence of wind farm, we can study the effect of different wind farm parameters on the static voltage stability by using these indexes.

1) *The effect of wind farm distance from network:*

Deciding where to install wind farm depends on various parameters such as presence of appropriate wind in that place. Therefore, accurately analyzing the effect of wind farm distance to its connection point to the network on static voltage stability is of great importance. To achieve this objective, wind farm was considered at 20, 40, and 60 kilometers distance from network and WFVSI and WFRPI indexes are calculated. Figure 9 shows WFSCI for these three conditions. The index has become more negative and the static voltage stability has been deteriorated. WFRPI index is shown in fig.10 also. This index appropriately shows the reactive power needed for different distances. For example, this index shows that how much reactive power at different wind speeds is needed to moderate the negative impact of line length increase on static voltage stability when the line length increases from 20 to 40 kilometers.

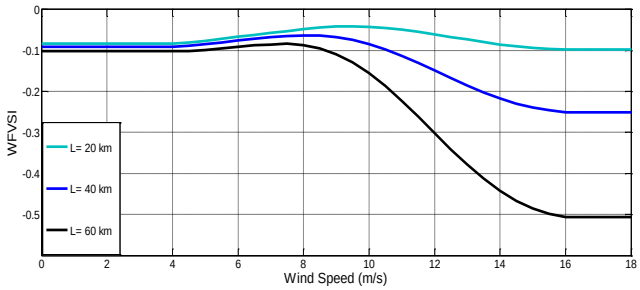

Fig. 9. WFVSI for different wind farm distances from the network

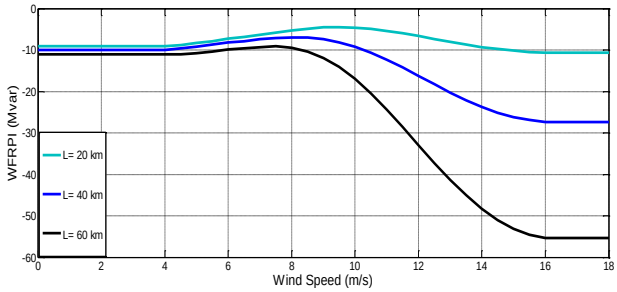

Fig. 10. WFRPI for different wind farm distances from the network

2) *The impact of different Wind Farm:*

Wind Farm Penetration Level $(WFPL)$ which is defined by (39) [16], as a fraction of total load (P_{Load}) served by wind farm generation (P_{WF}) is one of very effective factors on static voltage stability.

$$\%WFPL = \frac{P_{WF}}{P_{Load}} \times 100\% \quad (39)$$

In order to investigate the impact of different wind farm penetration levels on static voltage stability, we gradually increase the number of wind farm turbines from 10 units (one by one) and obtain WFVSI and WFRPI at different penetration levels. Fig. 11 indicates that in low penetration levels of wind farm the index is close to zero and wind farm has almost no effect on static voltage stability. The more the number of wind farm units, the worse is voltage stability of the network, because in this condition, the wind farm requires more reactive power from the network and the different bus voltages decrease and the collapse occurs, particularly, at bus which is connected to wind farm.

WFRPI index is shown at different wind farm penetrations in fig. 12. From this index we can obtain the reactive power needed to compensate the negative impact of wind farm on static voltage stability at different penetration levels.

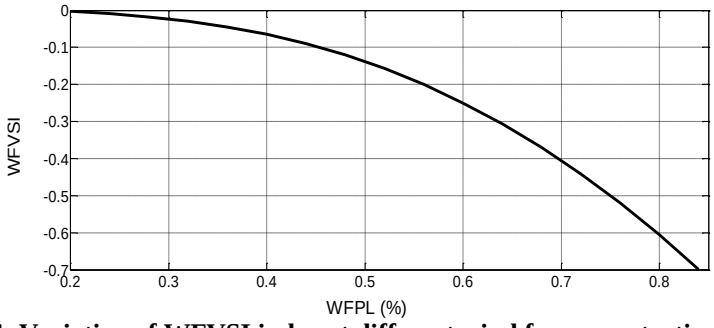

Fig.11. Variation of WFVSI index at different wind farm penetration levels

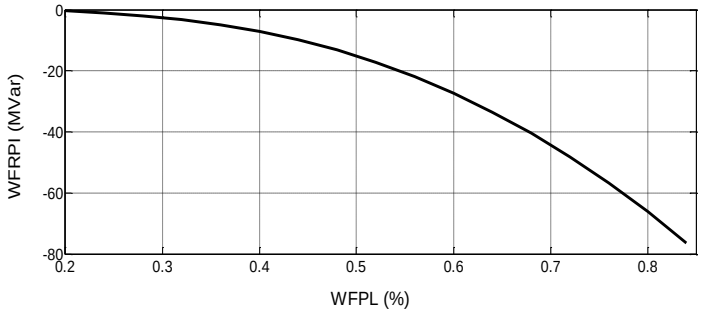

Fig. 12.Variation of WFRPI index at different wind farm penetration levels

3) *Effect of X/R Variation on WFRPI index:*

X/R ratio is one of the important parameters in stability of power systems. To investigate the effect of this ratio on static voltage stability, it has been varied from 1 to 13 and by doing so we obtained WFVSI and WFRPI indexes. Figure 13 shows that the increase in X/R ratio has deteriorated the static voltage stability.

.

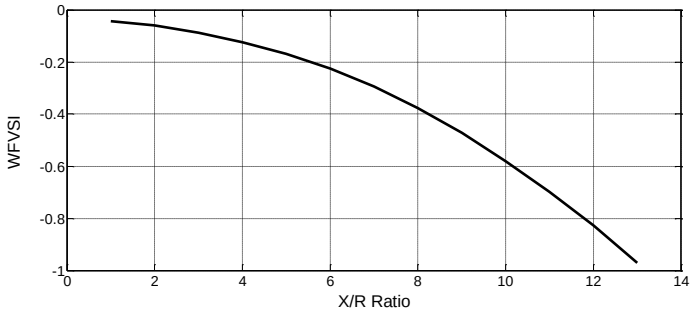

Fig. 13. Variation of WFVSI versus X/R ratio of wind farm connection line to the network

Fig. 14 provides reactive power requirements for the owners of wind farm and network operator at different X/R ratios. Therefore, the increase in X/R ratio imposes more costs to compensate the reactive power of the network.

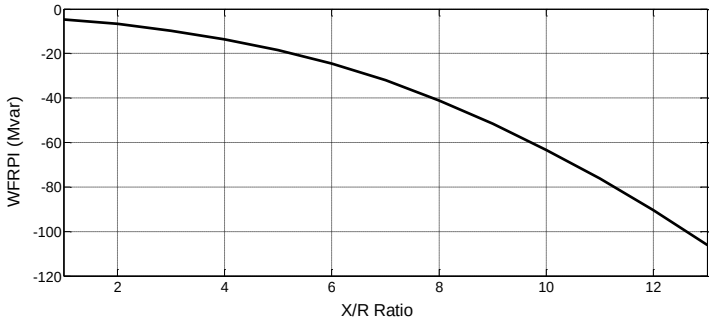

Fig.14. variation of WFRPI with X/R ratio

IV. CASE STUDY INVESTIGATION AND RESULTS

In this section, the effect of the presence of wind farm on static voltage stability of a standard test system is investigated. The under-study system in this section is IEEE standard 9-bus system. This system includes 9 buses, 3 generators, 6 lines, 3 transformators and 3 central loads. The information related to 9-bus system in base of 100 kVA is given in references [14, 15]. A wind farm with aforementioned specifications is connected in bus 9 of the system (see fig.15). Wind farm parameters are given in appendix.

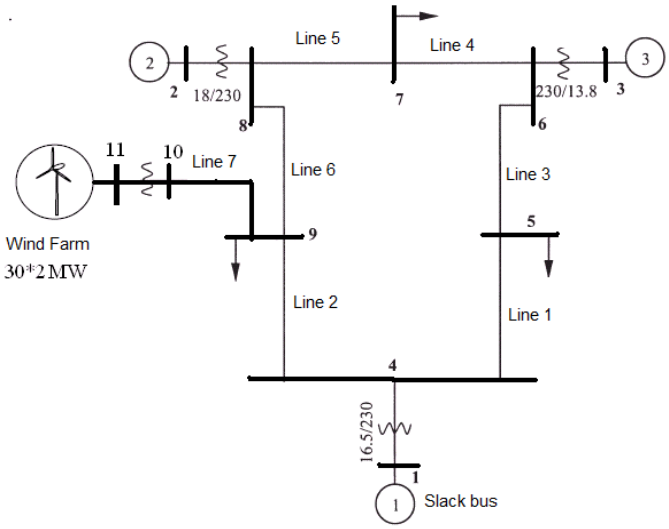

Fig. 15. IEEE standard 9 bus system with wind farm connection

The maximum loading of the system before and after connecting wind farm at different wind speeds was obtained through programming in MATLAB environment. In this program, the system's active and reactive load increase from the base load to collapse point according to equations (40) and (41):

$$P_{Li} = P_{L0}(1+\lambda) \quad (40)$$

$$Q_{Li} = Q_{L0}(1+\lambda) \quad (41)$$

In the above equations, P_{L0} and Q_{L0} are active and reactive base loads of the system, respectively.

Figure 16 shows the variation of WFVSI index for under study system. At this condition, the index is negative at all wind speeds; it means that wind farm in this condition has negative impact on voltage stability, particularly, at speeds close to nominal wind speed it has caused even more instability in system voltage.

Also, connecting wind farm to bus 9 of the system has had negative impact on voltage stability of the system, causing voltage instability at lower loading. WFVSI index is shown in figure 17. This index shows the difference between the critical reactive powers of the system with and without the presence of wind farm at different wind speeds. It can be observed that the difference of critical reactive powers in nominal wind speed is higher than its difference at other wind speeds.

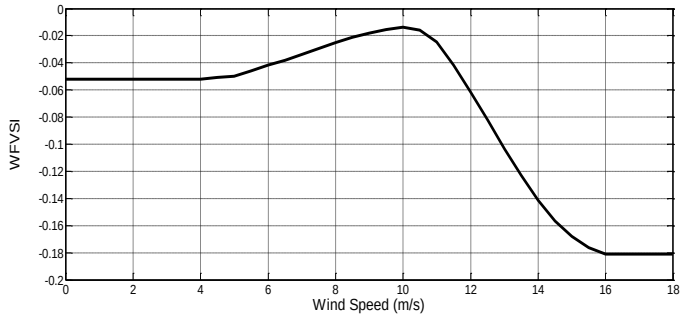

Fig. 16. WFVSI variations of the system according to wind speed

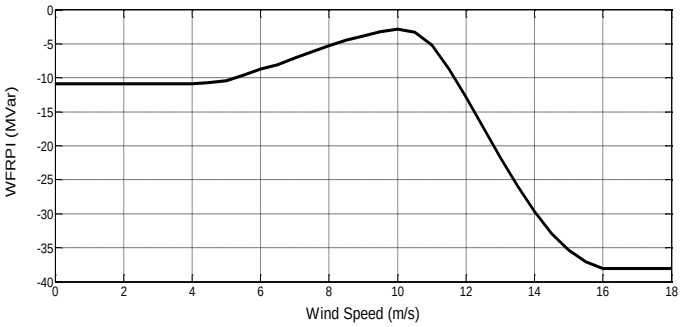

Fig. 17. WFRPI variations of the system according to wind speed

A. *System The effect of length of wind farm connection line to the network on voltage stability*

The distance of wind farm from the network is determined by the wind farm installation cite which itself depends on some factors such as existence of appropriate wind potential in that area. The effect of length of wind farm connection line to the network on voltage stability is investigated in this section. Figure 18 shows maximum loading parameter curves of the system at different wind speeds for 3 lengths of line, 20, 40 and 60 km. When wind farm is installed at further distances and the length of wind farm tie line to the network is increased, voltage instability of the system occurs at lower loads. The WFVSI curves of the system for different distances of wind farm from the network are shown in figure 19. As it could be observed, as wind farm distance from the network increases, WFVSI index becomes more negative and it shows that as wind farm distance from the network increases, particularly at speeds about nominal wind speed, there would be more negative impact on static voltage stability. Therefore, in order to prevent static voltage stability, particularly in distant wind farms, the network should enjoy enough reactive power resources. The diagrams of figure 20 that show WFRPI indexes for different distances of wind farm, provide the network owners with reactive power requirements for compensation at different wind speeds.

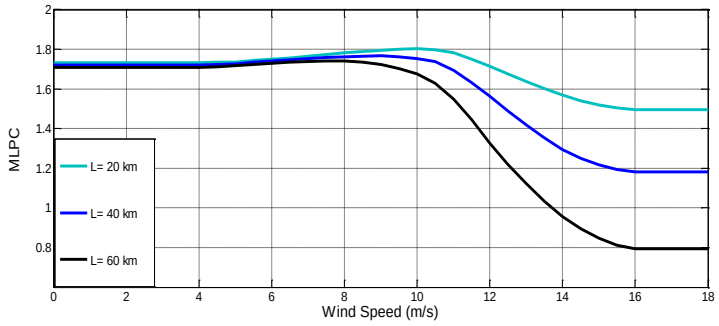

Fig. 18. Maximum loading parameter curves of the system for different distances of wind farm from the network

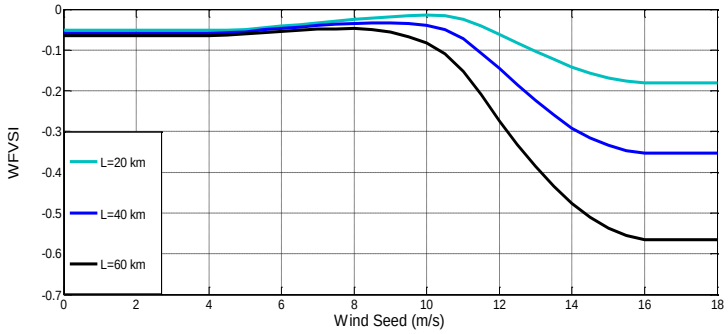

Fig. 19. WFVSI curves of the system for different distances of wind farm from the network

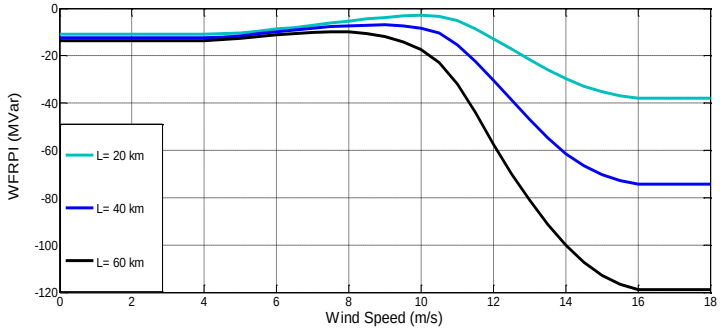

Fig. 20. WFRPI curves of the system for different distances of wind farm from the network

B. *Investigating different penetration levels of wind farm on static voltage stability*

To study the impact of different wind farm penetration levels on voltage stability of the network, a wind farm with different installed capacity 60, 100, and 140 MW (that are equivalent to 19, 32, and 44 percent penetration levels respectively) is connected to bus 9 of the system via a 20 km line. Maximum loading parameter curves of the system for different penetration levels of wind farm are shown in fig. 21. It can be observed that as wind farm penetration level increases, system loading decreases and this decrease is very tangible at nominal wind. When penetration level of wind farm reaches 44% at nominal wind speed, voltage instability in base load occurs at $\lambda_{\max} = 0$. As could be observed in figure 22, WFVSI curves have larger negative numbers in high penetration levels of wind farm. Therefore, voltage instability might cause problem in system utilization in high penetrations of wind power in power systems. If reactive power is insufficient in such systems, as power demand increases, the system would be at risk of voltage instability. Therefore, as wind power penetration level increases in future power systems, the study of static voltage stability becomes more important. Fig. 23 shows WFRPI curves for different penetration levels of wind farm.

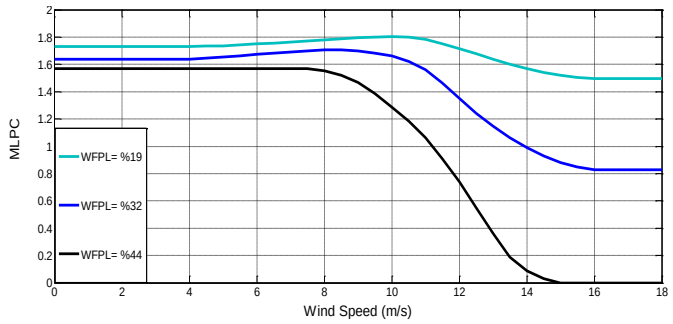

Fig. 21. Maximum loading parameter curves of the system for different penetration levels of wind farm

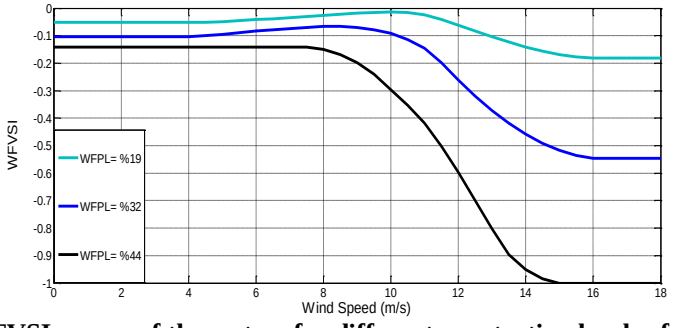

Fig. 22. WFVSI curves of the system for different penetration levels of wind farm

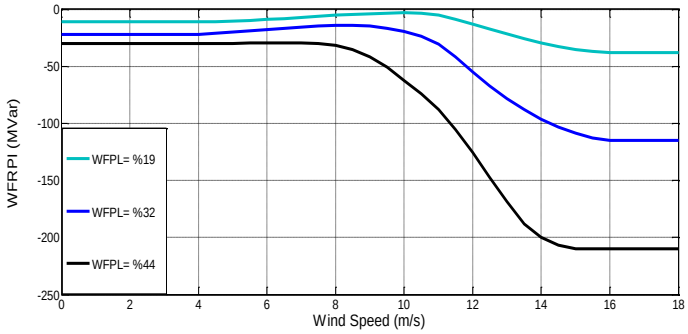

Fig. 23. WFRPI curves of the system for different penetration levels of wind farm

C. *The impact of wind farm penetration cite to the network on static voltage stability*

The impact of wind farm penetration level at different buses of the system on static voltage stability is investigated in this section. To achieve this objective, two wind farms with 60 and 140 MW nominal capacities were modeled and connected to different buses of the system.

1) *60 MW wind farm:*

Figure 24 shows maximum loading parameter of the system, connection cite of this farm, and wind speed. The voltage stability state of the system for connecting wind farm to different buses is shown very appropriately in this figure. It can be observed that voltage stability state of the system at all wind speeds, in case wind farm is connected to buses 6, 7, and 8 is better than when it is connected to buses 5 and 9. Furthermore, in case that wind farm is connected to bus 9 (the weakest bus of the system in terms of voltage stability), the system will have worst condition in terms of voltage stability. WFVSI is shown according to wind farm connection cite and wind speed in figure 25. This figure shows precisely how much is the impact of different connection cites of wind farm on static voltage stability. Having such pooches helps wind farm owners to prioritize wind farm connection cites to the network in terms of voltage stability and to design a system with appropriate stability. This figure shows that as wind farm is connected to buses 6, 7, and 8, stability state of the system, particularly at nominal speed will have significant improvement. The reactive power status of the system is shown in figure 16. This pooch can provide wind farm owners and network operator with reactive power required for compensation or reactive power reserved due to connecting wind farm to different cites of the system. Here, we add this point that connecting wind farm to each of buses of the system is with the supposition of existence of appropriate wind potential at given zone.

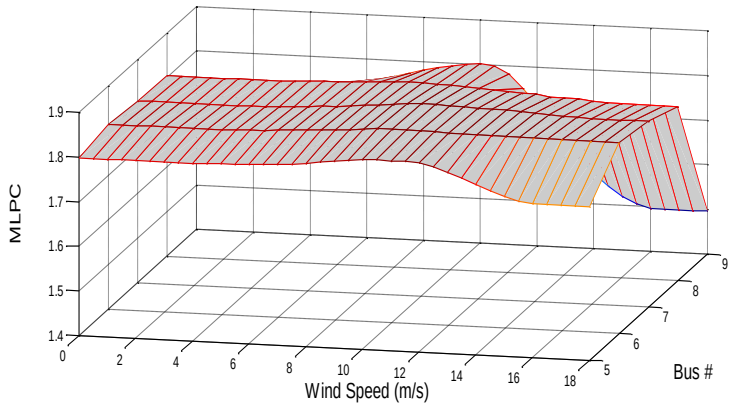

Fig. 24. Maximum loading parameter of the system according to 60 MW wind farm and wind speed

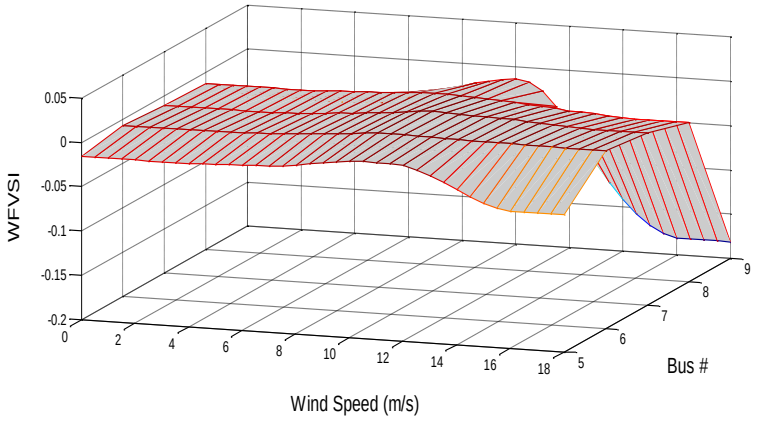

Fig. 25. WFVSI variations according to connection cite of 60 MW wind farm and wind speed

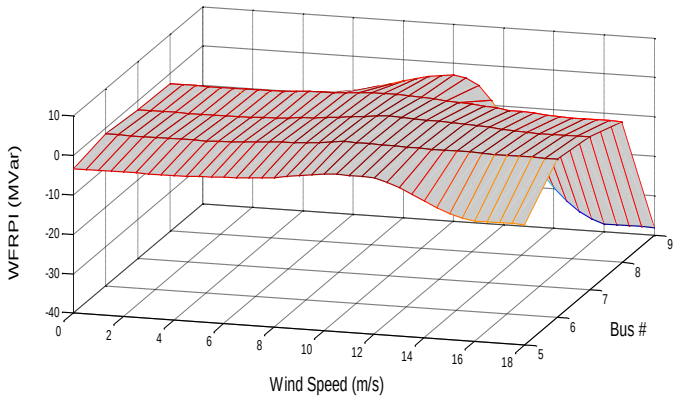

Fig. 26. WFRPI variations according to connection cite of 60 MW wind farm and wind speed

2) *140 MW wind farm:*

Figure 27 shows the pooch related to maximum loading parameter of the system for 140 MW wind farm. It could be observed that as wind farm penetration increases, bus 7 would be in inappropriate state in addition to buses 5 and 9. Therefore, reactive generation power of wind farm should be taken into consideration when selecting appropriate bus to connect to wind farm. For instance, bus 7 could be appropriate for connecting small wind farm in terms of voltage stability in the under-study system, while this bus is not appropriate for connecting a bigger wind farm. The pooch related to WFVSI for different connection cites of wind farm is shown in figure 28. This index introduces buses 6 and 8 as candidate buses for connecting wind farm. Reactive power required, in case wind farm is connected to each of the buses is calculable in WFRPI index which is shown in figure 29. Regarding this figure, if wind farm is connected to buses 5 and 9, big capacitor banks would be needed to improve voltage stability.

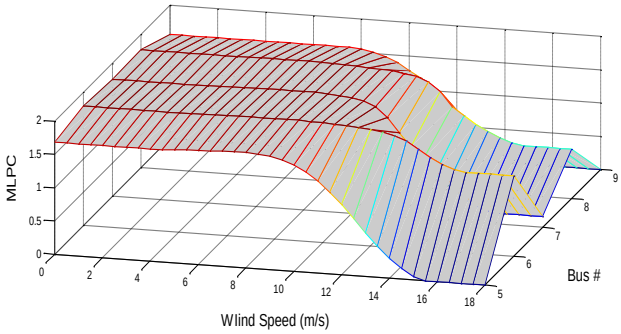

Fig. 27. Maximum loading parameter of the system according to connection cite of 140 MW wind farm and wind speed

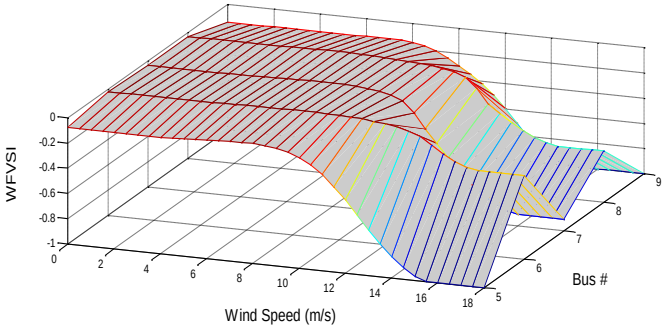

Fig. 28. WFVSI variations according to connection cite of 140 MW wind farm and wind speed

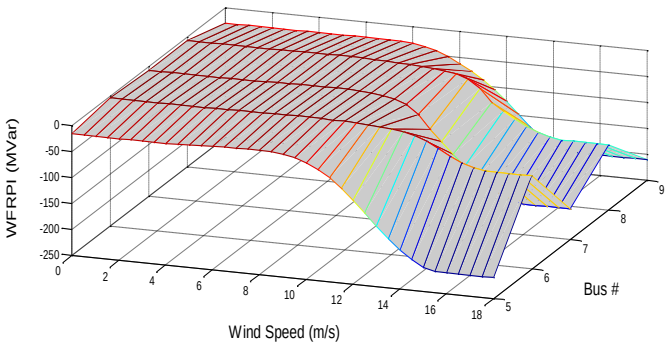

Fig. 29. WFRPI variations according to connection cite of 140 MW wind farm and wind speed

V. CONCLUSIONS

As penetration level of wind turbines equipped with SCIG increases in power systems, voltage stability of the system is influenced mach more. The results show that maximum loading of power system is a function of wind speed. Voltage instability of the system in many conditions occurs at lower loading compared to without wind farm state. Also, the presence of wind farm has more negative impact on voltage stability of system in nominal wind speed. In order to precisely evaluating the impact of wind farm on voltage stability of the system, new indexes were introduced. The impact of different parameters on voltage stability was investigated using these indexes. The results show that as the length of wind farm connection cite to the network and wind farm penetration level increase, voltage stability status of the system deteriorates. Furthermore, it was shown that as wind farm is connected to weak bus of the system (bus 9 in under-study system), voltage stability status deteriorates.

VI. APPENDIX

The study system parameters are given next.

Table 1. Wind farm parameters in base of 100 kVA induction generator

parameters	pu
R_r	0.01(pu)
R_s	0.01(pu)
X_r	0. 1(pu)
X_s	0. 08(pu)
X_m	3(pu)

REFERENCES

[1] Department of Energy, "20% Energy by 2030: Increasing Wind Energy's Contribution to U.S. Electricity Supply", Washington, DC, July 2008

[2] E. Vittal, M. O'Malley and A. Keane, "ASteady-State Voltage Stability Analysis of Powe Systems With High Penetrations of Wind", IEEE TRANS, VOL. 25, NO. 1, FEB 2010, PP. 433-442.

[3] I.S. Naser, A. Garba, O. Anaya-Lara and K.L. Lo, "Voltage stability of transmission network with different penetration levels of wind generation", (UPEC), 2010, 45th International, Sept, 2010, PP1-5.

[4] Anca D. Hansen, Lars H. Hansen, " Market penetration of wind turbine concepts over the years", EWEC,May. 2007, pp:1-10.

[5] Thomas Ackermann, "Wind Power in Power Systems", John Wiley and Sons Ltd, 2005.

[6] NAJAFI. Hamid Reza, ROBINSON. Francis, DASTYAR. Farshad and SAMADI. Ali Asghar, "Small-Disturbance Voltage Stability of Distribution Systems with wind turbine implemented with wound rotor Induction Generators", accepted in IEEE conference, Lisbon, Portugal, march 2009.

[7] J. Wiik, J.O. Gjefde, T. Gjengedal, "Impacts from large scale integration of wind energy farms into weak power systems", Proceedings of Power Con 2000, Perth, December 4-7, 2000, v.1, pp.49 -54.

[8] J.G. Slootweg, W.L. Kling, "Modelling and analysing impacts of wind power on transient stability of power systems", Wind Engineering, v.26, n.1, 2002, pp.3-20.

[9] J.G. Slootweg, S.W.H. de Haan, H. Polinder and W.L. Kling, "Simulation of electrical power systems with a high wind energy penetration", Proceedings of the IEA R&D Wind Topical Expert Meeting on Large Scale Integration into the Grid, November 6-7,
2001, Hexham UK, pp.113-126.

[10] A. Feijoo and J. Cidras "Modeling of wind farms in the load flow analysis", IEEE Trans, 15, VOL.15, NO.1,PP. 110–116, 2000.

[11] KC. Divya and PSN. Rao, "Models for wind turbine generating systems and their application in load flow studies", Electric Power Systems Research, VOL.76, PP. 844–856, 2006.

[12] TV. Cutsem, C. Vournas, "Voltage stability of electric power systems", Boston: Kluwer Academic Publishers Springer; 1998.

[13] U. Eminoglu, "Modeling and application of wind turbine generating system (WTGS) to distribution systems", Elsevier Ltd, Nigde University, Nigde, Turkey, PP: 2474–2483, 2009.

[14] "Power System Analysis Toolbox (PSAT)", Version 1.3.4, July 14, 2005.

[15] P.M. Anderson and A.A. Fouad, "Power System Control and Stability", Galgotia publications, 1981.

[16] N. HEMDAN M. KURRAT "Influence of Distributed Generation on Difference Loadablity Aspects of Electric Distribution Systems", 20th International Conference on Electricity Distribution, Paper No.0255, 8-11 June 2009.

